THE JOURNAL OF PHYSICAL CHEMISTRY B

Article

pubs.acs.org/JPCB

# Ionic Liquid Effects on Nucleophilic Aromatic Substitution Reactions from QM/MM Simulations

Caley Allen, Billy W. McCann, and Orlando Acevedo*

Department of Chemistry and Biochemistry, Auburn University, 179 Chemistry Building, Auburn, Alabama 36849, United States

Supporting Information

**ABSTRACT:** Nucleophilic aromatic substitution ($S_NAr$) reactions are particularly sensitive to medium effects and have been reported to benefit from ionic liquids. The $S_NAr$ reaction between cyclic secondary amines (i.e., piperidine, pyrrolidine, and morpholine) and the 2-L-5-nitrothiophene (para-like) and 2-L-3-nitrothiophene (ortho-like) isomers, where L = bromo, methoxy, phenoxy, and 4-nitrophenoxy, has been computationally investigated in 1-butyl-3-methylimidazolium tetrafluoroborate and hexafluorophosphate [BMIM][$BF_4$] and [BMIM][$PF_6$], respectively. QM/MM Monte Carlo simulations utilizing free-energy perturbation theory were used to characterize the solute−solvent interactions over the addition−elimination reaction pathway. Energetic and structural analyses determined that the improved $S_NAr$ reactivity in [BMIM][$BF_4$] and [BMIM][$PF_6$] can be attributed to (1) an enhanced nucleophilicity of the cyclic amines in the ionic liquids with an order of Pyr ≥ Pip > Mor, (2) beneficial $\pi^+-\pi$ interactions between the BMIM cations and the aromatic rings present on the substrate that enhanced coplanarity between the thiophene ring and the aromatic substituents, resulting in a larger positive charge on the reacting ipso carbon, and (3) a highly ordered ionic liquid clathrate formation that, despite an entropy penalty, provided reduced activation free-energy barriers derived from an increasing number of solvent ions favorably interacting with the emerging charge separation at the rate-limiting addition step.

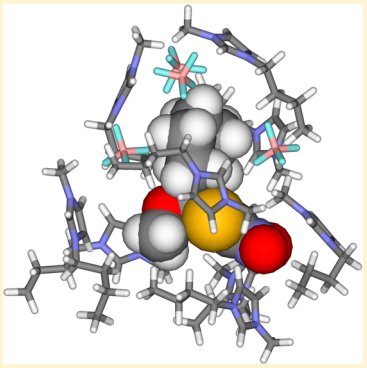

## INTRODUCTION

Ionic liquids are molten salts characteristically at room temperature.[1] Cations can be fine-tuned through various functional groups to enhance the degree of localized structuring with the anions in the liquid phase.[2,3] Consequently, different ion combinations can dramatically alter solvent properties, including the melting point, viscosity, density, electrical conductance, solvent polarity, and gas solubility.[4,5] As a medium for chemical reactions, the ionic liquids 1-butyl-3-methylimidazolium tetrafluoroborate and hexafluorophosphate, [BMIM][$BF_4$] and [BMIM][$PF_6$], respectively, have gained significant popularity due to their ideal properties in catalysis[6−8] and organic synthesis.[9−11] For example, nucleophilic aromatic substitution ($S_NAr$) reactions, which can be particularly sensitive to medium effects,[12,13] have been reported to derive sizable rate enhancements from the ionic liquids [BMIM][$BF_4$] and [BMIM][$PF_6$] relative to conventional solvents.[14,15]

Of particular interest is the $S_NAr$ reaction reported by D'Anna et al. between cyclic secondary amines (AmH) and the 2-L-5-nitrothiophene (para-like) or 2-L-3-nitrothiophene (ortho-like) isomers (Scheme 1).[14] Experimental rates and thermodynamics are available in multiple ionic liquids for three nucleophiles, that is, piperidine, pyrrolidine, and morpholine (Scheme 2), and four leaving groups: L = bromo, methoxy, phenoxy, and 4-nitrophenoxy. The $S_NAr$ reaction follows an addition−elimination mechanism, where nucleophilic attack on the ipso carbon forms an intermediate Meisenheimer complex followed by cleavage of the C−L bond. In methanol, the reaction proceeds via an uncatalyzed pathway, $k_{obs} = k_1[AmH]$, due to the solvent's ability to stabilize the transition state.[16] Because imidazolium-based

**Scheme 1. Addition−Elimination Mechanism between 2-L-5-Nitrothiophene (para-like) or 2-L-3-Nitrothiophene (ortho-like) Isomer and a Cyclic Amine (AmH) Involving the Formation of an Intermediate Meisenheimer Complex[a]**

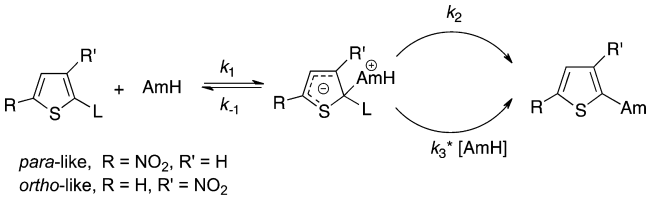


[a]Leaving groups are L = Br, $OCH_3$, $OC_6H_5$, and $OC_6H_4$-4-$NO_2$.

**Scheme 2. Cyclic Amine Nucleophiles: Piperidine (Pip), Pyrrolidine (Pyr), and Morpholine (Mor)**

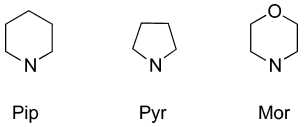


**Special Issue:** William L. Jorgensen Festschrift

**Received:** May 20, 2014
**Revised:** July 10, 2014

   dx.doi.org/10.1021/jp504967r | J. Phys. Chem. B XXXX, XXX, XXX−XXX

ionic liquids can act as a simultaneous hydrogen bond donor and acceptor, the $S_NAr$ reaction is postulated to behave in a similar fashion in the molten salts. Interestingly, the ortho-like isomer possesses an intramolecular interaction between the nitro group and the amine proton that can behave equivalently to protic solvents at the transition state regardless of the reaction medium, for example, in benzene.[17] Our previous computational work on Kemp decarboxylations used a similar "built-in solvation" approach to elucidate information about rate dependence upon hydrogen bonding.[18]

Combined quantum and molecular mechanical (QM/MM) calculations utilizing Monte Carlo statistical mechanics and free-energy perturbation theory (MC/FEP) have been carried out for the thiophene-based reactions in the [BMIM][$BF_4$] and [BMIM][$PF_6$] ionic liquids and in methanol. Activation barriers, solute−solvent interactions, and amine nucleophilicity have been computed to further explore the effect of these molten salts upon the $S_NAr$ reaction. Comparisons are made to density functional theory (DFT) calculations using an implicit continuum model for methanol. This work provides new insights into the effect of ionic liquids upon an important organic reaction, which can help predict optimal conditions for other reactions in addition/elimination classes.

## COMPUTATIONAL METHODS

The $S_NAr$ reactions were examined using QM/MM calculations that employed the PDDG/PM3 semiempirical QM method[19−21] to treat the reacting systems, Metropolis Monte Carlo sampling, and free-energy perturbation theory. PDDG/PM3 has been successfully applied to multiple solution-phase QM/MM chemical reaction studies,[22−24] including a previous $S_NAr$ reaction between an azide ion and 4-fluoronitrobenzene.[13] In addition, the method has accurately reproduced experimental results for reactions in ionic liquids including the Diels−Alder reaction,[25,26] the Kemp elimination,[27] and a $\beta$-elimination.[28] The computation of the QM energy and atomic charges was performed for each attempted move of the solute, which occurred every 100 configurations. Partial charges were obtained from the CM3 charge model[29] and scaled by 1.14 to reflect the polarization in a condensed-phase environment. In addition to the electrostatic contributions to the solute−solvent energy, Lennard-Jones interactions between solute and solvent atoms were taken into account using OPLS parameters. This combination has been found to minimize errors in the computed free energies of hydration when using a PM3-based method.[30]

Periodic boundary conditions were applied to tetragonal boxes containing the solutes plus 188 ion pairs for the ionic liquids or 390 solvent molecules for methanol. All solvents were represented explicitly using our custom OPLS-AA force field,[27] and long-range electrostatic interactions were treated with Ewald summations. The ionic liquid cations were fully flexible, meaning that all bond stretching, angle bending, and torsional motions were sampled with MC. Anions were simulated as rigid molecules. The use of rigid anions in OPLS-AA has been shown to provide an accurate representation of ionic-liquid physical properties, including the solvent effects for the previously stated QM/MM reaction studies. Solute−solvent and solvent−solvent intermolecular cutoff distances of 12 Å were used for the tail carbon atom of each side chain, a midpoint carbon on the butyl chain, and the ring carbon between both nitrogens. Center atoms, for example, B in $BF_4^-$ and P in $PF_6^-$, were used for the anions. If any distance was within the cutoff, the entire solvent−solvent interaction was included. Adjustments to the allowed ranges for rotations, translations, and dihedral angle movements led to overall acceptance rates of ∼30% for new configurations. Simulations were performed using an NPT ensemble at 25 °C and 1 atm. FEP windows were run simultaneously on computers located at Auburn University and the Alabama Supercomputer Center.

The starting geometries for the solutes were determined by executing a MC conformational search that resulted in up to 100 unique structures. The top 10 most favorable MC structures were then recomputed with B3LYP/6-311++G(2d,p) geometry optimizations using Gaussian 09.[31] The resultant lowest energy structure was employed as the starting geometry for the QM/MM calculation. The effect of solvent was also explored by using the integral equation formalism variant of the polarizable continuum model (IEF-PCM) with the UFF cavity.[32] Frequency calculations were performed to verify all stationary points as minima for ground states or as saddle points for transition structures.

## RESULTS AND DISCUSSION

**Energetics and Geometries.** The $\Delta G^{\ddagger}$ for the $S_NAr$ reaction was computed by perturbing the $R_{CN}$ distance between the reacting ipso carbon of the solute and the amine nitrogen in increments of 0.02 Å from the equilibrium bond distance in the Meisenheimer complex to a 5 Å separation that represents the noninteracting reactants (Scheme 3). While 2.5 and 5 million

**Scheme 3. Procedure for Calculating the $S_NAr$ Reaction Free Energy Surface**

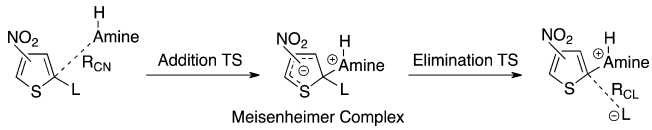


MC configurations of equilibration and averaging, respectively, sufficed for the methanol simulations, the extensive reorganization required for the ionic liquids resulted in an increased 160 and 20 million configurations, respectively, per FEP window. Because of the large computational demands in the ionic liquid simulations, that is, 175 FEP windows per reaction, the experimentally determined rate-limiting addition step[14] was the focus of the calculations. The distance between the leaving group and the ipso carbon, $R_{CL}$, was variable in the addition step. However, $R_{CL}$ could be used, in principle, to compute the elimination transition structure (Schemes 3 and 4) and is

**Scheme 4. Alternative Procedures for Calculating the $\Delta G^{\ddagger}$ for the Elimination Step**

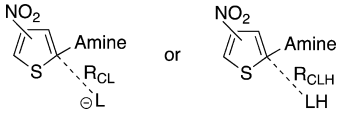


discussed further later. The QM/MM calculated $\Delta G^{\ddagger}$ in the ionic liquids provided reasonable barriers that were overestimated in some cases (Table 1). The error bars in the ionic liquids simulations are estimated at ±1.5 kcal/mol, and experimental error bars are reported to be as large as ±1 kcal/mol.[14] A cratic entropy correction of 1.89 kcal/mol was included in the final energy values.[33]


dx.doi.org/10.1021/jp504967r | J. Phys. Chem. B XXXX, XXX, XXX−XXX

**Table 1. Free Energy of Activation, $\Delta G^{\ddagger}$ (kcal/mol), Calculated at 25 °C for the $S_NAr$ Reactions between the 2-L-3-Nitrothiophene (Ortho-like) and 2-L-5-Nitrothiophene (Para-like) Isomers and Three Cyclic Amines in Methanol and Ionic Liquids[a,b]**

| nucleophile | thiophene derivative | leaving group (L) | $\Delta G^{\ddagger}$ $CH_3OH$[c] | $\Delta G^{\ddagger}$ DFT $CH_3OH$[d] | $\Delta G^{\ddagger}$ [BMIM][$BF_4$][c] | $\Delta G^{\ddagger}$ [BMIM][$PF_6$][c] |
|---|---|---|---|---|---|---|
| morpholine | ortho-like | Br | 26.0 | 30.7 | 27.9 (23.7) | 26.5 |
| | | $OCH_3$ | 24.4 | 31.0 | 25.1 | 25.9 |
| | | $OC_6H_5$ | 21.4 | 29.0 | 28.5 | 27.8 |
| | | $OC_6H_4$-4-$NO_2$ | 22.4 | 28.6 | 27.8 | 23.8 |
| | para-like | Br | 26.2 (26.7) | 32.5 | 25.0 (24.5) | 27.5 |
| | | $OCH_3$ | 27.3 | 32.7 | 30.0 | 26.6 |
| | | $OC_6H_5$ | 26.2 | 33.1 | 27.3 (23.8) | 28.5 |
| | | $OC_6H_4$-4-$NO_2$ | 26.0 | 31.6 | 28.0 (23.3) | 28.6 |
| piperidine | ortho-like | Br | 25.1 (24.8) | 28.7 | 23.5 (22.5) | 22.8 |
| | | $OCH_3$ | 24.5 | 29.1 | 27.3 | 24.0 |
| | | $OC_6H_5$ | 23.2 | 27.3 | 24.8 | 24.0 |
| | | $OC_6H_4$-4-$NO_2$ | 22.1 | 26.8 | 25.4 | 21.1 |
| | para-like | Br | 25.7 (26.0) | 30.8 | 25.8 (23.0) | 25.1 |
| | | $OCH_3$ | 26.5 (23.6) | 30.7 | 27.6 (21.8) | 26.2 |
| | | $OC_6H_5$ | 25.1 | 30.5 | 23.8 (22.1) | 26.0 |
| | | $OC_6H_4$-4-$NO_2$ | 24.5 (24.1) | 29.4 | 24.1 (21.5) | 29.1 |
| pyrrolidine | ortho-like | Br | 24.0 (24.3) | 28.8 | 25.1 (21.7) | 27.7 |
| | | $OCH_3$ | 22.5 | 29.5 | 23.6 | 25.6 |
| | | $OC_6H_5$ | 20.3 | 27.0 | 26.7 | 25.1 |
| | | $OC_6H_4$-4-$NO_2$ | 19.7 | 26.9 | 21.7 | 22.6 |
| | para-like | Br | 25.7 (25.7) | 30.8 | 28.6 (22.8) | 23.9 (23.2) |
| | | $OCH_3$ | 24.9 | 31.1 | 28.8 (21.2) | 26.4 |
| | | $OC_6H_5$ | 24.2 | 31.1 | 26.1 (21.8) | 25.5 |
| | | $OC_6H_4$-4-$NO_2$ | 23.3 | 29.4 | 25.1 (21.3) | 23.7 |

[a]Experimental energies are given in parentheses. [b]Ref 14. [c]PDDG/PM3/OPLS-AA and MC/FEP. [d]DFT = B3LYP/6-311++G(2d,p)/PCM optimization.

**Table 2. QM/MM/MC Calculated $R_{CN}$ Bond Distances (angstroms) for the Addition Step Transition Structures in Solution[a]**

| nucleophile | thiophene derivative | leaving group (L) | $R_{CN}$ $CH_3OH$ | $R_{CN}$ DFT $CH_3OH$[b] | $R_{CN}$ [BMIM][$BF_4$] | $R_{CN}$ [BMIM][$PF_6$] |
|---|---|---|---|---|---|---|
| morpholine | ortho-like | Br | 2.02 | 1.96 | 2.00 | 1.94 |
| | | $OCH_3$ | 1.96 | 1.98 | 1.92 | 1.84 |
| | | $OC_6H_5$ | 1.96 | 1.95 | 1.92 | 1.88 |
| | | $OC_6H_4$-4-$NO_2$ | 2.00 | 1.95 | 1.92 | 1.96 |
| | para-like | Br | 1.98 | 1.91 | 1.92 | 1.94 |
| | | $OCH_3$ | 1.92 | 1.92 | 1.88 | 1.80 |
| | | $OC_6H_5$ | 1.96 | 1.87 | 1.88 | 1.80 |
| | | $OC_6H_4$-4-$NO_2$ | 1.92 | 1.88 | 1.76 | 1.92 |
| piperidine | ortho-like | Br | 2.00 | 1.93 | 2.00 | 2.04 |
| | | $OCH_3$ | 1.98 | 2.03 | 1.94 | 1.98 |
| | | $OC_6H_5$ | 2.00 | 2.00 | 1.96 | 1.92 |
| | | $OC_6H_4$-4-$NO_2$ | 2.02 | 2.01 | 2.04 | 1.96 |
| | para-like | Br | 1.96 | 1.92 | 1.82 | 1.92 |
| | | $OCH_3$ | 1.94 | 1.97 | 1.96 | 1.92 |
| | | $OC_6H_5$ | 1.92 | 1.93 | 1.88 | 1.94 |
| | | $OC_6H_4$-4-$NO_2$ | 1.91 | 1.93 | 1.88 | 1.80 |
| pyrrolidine | ortho-like | Br | 2.03 | 2.02 | 2.00 | 1.94 |
| | | $OCH_3$ | 2.08 | 2.02 | 2.02 | 1.84 |
| | | $OC_6H_5$ | 2.00 | 2.01 | 1.92 | 1.96 |
| | | $OC_6H_4$-4-$NO_2$ | 2.02 | 2.01 | 2.08 | 2.02 |
| | para-like | Br | 1.98 | 1.97 | 1.94 | 1.92 |
| | | $OCH_3$ | 1.96 | 1.99 | 1.80 | 1.72 |
| | | $OC_6H_5$ | 1.94 | 1.94 | 1.98 | 1.96 |
| | | $OC_6H_4$-4-$NO_2$ | 1.94 | 1.94 | 1.94 | 1.96 |

[a]PDDG/PM3/OPLS-AA and MC/FEP. [b]DFT = B3LYP/6-311++G(2d,p)/PCM optimizations.

The QM/MM calculated $\Delta G^{\ddagger}$ for the addition step in methanol provided good agreement when compared with experiment (Table 1). For example, the $S_NAr$ reaction between morpholine and 2-bromo-5-nitrothiophene yielded a computed $\Delta G^{\ddagger}$ of 26.2 kcal/mol (exptl 26.7 kcal/mol). Error bars in the free-energy barriers in methanol were calculated by propagating


dx.doi.org/10.1021/jp504967r | J. Phys. Chem. B XXXX, XXX, XXX−XXX

**Table 3. Free Energy of Activation, $\Delta G^{\ddagger}_{reverse}$ (kcal/mol), at 25 °C for the Reverse $S_NAr$ Reaction From the Meisenheimer Intermediate to the Reactants for the 2-L-3-Nitrothiophene (ortho-like) and 2-L-5-Nitrothiophene (para-like) Isomers and Three Cyclic Amines in Solution[a]**

| nucleophile | thiophene derivative | leaving group (L) | $\Delta G^{\ddagger}_{reverse}$ $CH_3OH$ | $\Delta G^{\ddagger}_{reverse}$ [BMIM][$BF_4$] | $\Delta G^{\ddagger}_{reverse}$ [BMIM][$PF_6$] |
|---|---|---|---|---|---|
| morpholine | ortho-like | Br | 10.4 | 9.5 | 10.3 |
| | | $OCH_3$ | 3.1 | 2.8 | 1.9 |
| | | $OC_6H_5$ | 6.3 | 3.2 | 3.7 |
| | | $OC_6H_4$-4-$NO_2$ | 8.0 | 5.6 | 4.2 |
| | para-like | Br | 9.2 | 10.4 | 9.6 |
| | | $OCH_3$ | 3.3 | 1.9 | 1.2 |
| | | $OC_6H_5$ | 3.6 | 1.4 | 1.6 |
| | | $OC_6H_4$-4-$NO_2$ | 5.1 | 1.0 | 2.0 |
| piperidine | ortho-like | Br | | 11.0 | 10.8 |
| | | $OCH_3$ | 6.0 | 3.3 | 4.4 |
| | | $OC_6H_5$ | 7.2 | 4.2 | 2.9 |
| | | $OC_6H_4$-4-$NO_2$ | 8.1 | 5.2 | 4.5 |
| | para-like | Br | 9.6 | 9.2 | 11.1 |
| | | $OCH_3$ | 4.9 | 5.2 | 3.0 |
| | | $OC_6H_5$ | 5.0 | 3.1 | 4.4 |
| | | $OC_6H_4$-4-$NO_2$ | 5.4 | 3.1 | 1.4 |
| pyrrolidine | ortho-like | Br | | 12.1 | 11.2 |
| | | $OCH_3$ | 9.9 | 8.6 | 4.4 |
| | | $OC_6H_5$ | 9.3 | 8.6 | 4.2 |
| | | $OC_6H_4$-4-$NO_2$ | 10.6 | 7.6 | 6.9 |
| | para-like | Br | 10.5 | 8.5 | 10.9 |
| | | $OCH_3$ | 5.2 | 3.3 | 1.4 |
| | | $OC_6H_5$ | 6.4 | 5.9 | 5.7 |
| | | $OC_6H_4$-4-$NO_2$ | 5.6 | 4.9 | 7.4 |

[a]PDDG/PM3/OPLS-AA and MC/FEP.

the standard deviation ($\sigma_i$) on each individual $\Delta G_i$ and resulted in overall uncertainties in the $\Delta G^{\ddagger}$ of ca. 0.4 kcal/mol. As a point of comparison, $\Delta G^{\ddagger}$ values computed for the $S_NAr$ reactions in methanol utilizing B3LYP/6-311++G(2d,p)/PCM were found to be overestimated relative to experiment. The previous example, that is, morpholine and 2-bromo-5-nitrothiophene, using DFT/PCM gave a $\Delta G^{\ddagger}$ of 32.5 kcal.

In preliminary calculations, when the $\Delta G^{\ddagger}$ for the elimination step was computed for L = Br using the $R_{CL}$ perturbation shown in Scheme 3, the facile ability of Br to stabilize a full negative charge led to lower energy barriers than the addition step. However, the leaving groups L = $OCH_3$, $OC_6H_5$, and $OC_6H_4$-4-$NO_2$ provided a more challenging calculation as the corresponding mechanism is more complex and can proceed via multiple routes, that is, $k_2$ and $k_3$*[AmH] (Schemes 1, 3, and 4). For example, the 2-(4-nitrophenoxy)-5-nitrothiophene DFT calculation spontaneously elongated in the Meisenheimer complex to abstract a proton from the amine consistent with a protonated leaving group in the elimination step ($R_{CLH}$ in Scheme 4). While the emphasis of this work is on the rate-limiting addition step, a detailed study of the elimination step with different leaving groups and in multiple solvents is of interest and will be the focus of future work.

The transition structure geometries for the $R_{CN}$ addition (±0.02 Å error) of the amine to the nitrothiophenes are given in Table 2 for all reaction combinations. A solvent dependence was noted, with the reaction in methanol generally yielding longer $R_{CN}$ bonds compared with the [BMIM][$BF_4$] and [BMIM][$PF_6$] ionic liquids. The difference in geometries may stem, in part, from steric differences for the solutes in methanol compared to the bulky cation in the ionic liquids. However, a major factor dictating geometry differences is the stabilization of emerging charges as the reaction proceeds toward the intermediate Meisenheimer complex. From examination of the QM/MM activation free energies for the reverse reaction from the Meisenheimer complex back to the reactants, $\Delta G^{\ddagger}_{reverse}$, it is clear that the transition states effectively resemble the Meisenheimer complex more closely in the ionic liquids than methanol (Table 3). The low values for $\Delta G^{\ddagger}_{reverse}$ in the ionic liquids are likely derived from a more favorable $\Delta S^{\ddagger}_{reverse}$ as the ionic liquids become highly ordered at the Meisenheimer intermediate (discussed later).

**$\pi^+$–$\pi$ Interactions.** Ionic liquids can provide unique and beneficial $\pi^+$–$\pi$ interactions between the BMIM cation and the substrate aromatic rings that can potentially enforce a coplanarity similar to what was reported for the $\beta$-elimination of 1,1,1-tribromo-2,2-bis(3,4-dimethoxyphenyl)ethane[28,34] and for ortho-substituted benzoic acid dissociations.[35] Monitoring the average dihedral angle, Φ, as defined in Figure 1, over the course of the simulation finds the geometry orientation of the phenoxy and 4-nitrophenoxy leaving groups to be somewhat dependent on the position of the $NO_2$ group. For example, the 2-L-3-nitrothiophene (ortho-like) systems favor a gauche conformation relative to the thiophene ring that reduces poor steric interactions between the bulky leaving group and the nitro group. However, the 2-L-5-nitrothiophene (para-like) transition state does not have the potential for unfavorable sterics and as such primarily occupies a trans configuration. Table 4 highlights these preferences in the piperidine-based reactions. (Supporting Information Table S1 provides dihedral angles for the morpholine- and pyrrolidine-based reactions.)

A coplanar orientation between the nitrothiophene ring and phenoxy rings should emphasize conjugation, potentially increasing the electron-withdrawing effect of the oxygen atom


dx.doi.org/10.1021/jp504967r | J. Phys. Chem. B XXXX, XXX, XXX−XXX

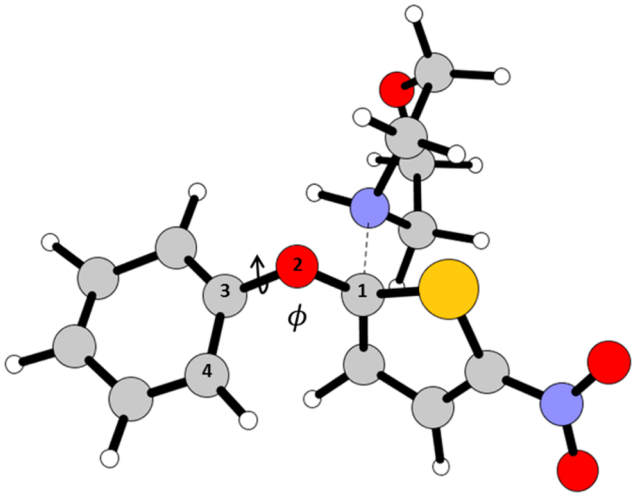


**Figure 1.** Snapshot of the transition state between morpholine and 2-phenoxy-5-nitrothiophene from the QM/MM/MC calculations. Φ = 360 − $\phi$(C1−O2−C3−C4)°.

bonded to the heteroaryl moiety. Interestingly, the transition states in [BMIM][$BF_4$] and [BMIM][$PF_6$] overcame the steric hindrance and adopted a trans alignment for ∼20% of the calculation. This ionic liquid effect may partially explain the origin of the observed rate enhancements in the ionic liquids.[14,15] However, the ortho-like isomer also possesses an intramolecular interaction between the nitro group and the amine proton that can behave equivalently to protic solvents at the transition state, negating much of the solvent effect differences, for example, in methanol versus benzene.[17]

Pi stacking interactions between the nitrothiophene ring and 4-nitrophenoxy substituent with the solvent BMIM cations were quantified by evaluating the average distances and angles between the approximated centers of the rings. A distance ($X$) and angle ($\theta$) connecting the two planes of the pi systems are defined in Figure 2. The $\pi^+-\pi$ interactions, that is, average $X$ and $\theta$ values over the final 20 million MC configurations, from the two nearest BMIM cations are reported in Table 5 for the transition states and intermediate Meisenheimer complexes in the reactions involving the three cyclic amines and the para-like and ortho-like reactants in [BMIM][$BF_4$]. All cation-substrate pi interactions in [BMIM][$BF_4$] and [BMIM][$PF_6$] that are within 9 Å are reported with standard deviations in Tables S2−S13 in the Supporting Information.

The calculations for the 2-(4-nitrophenoxy)-5-nitrothiophene (para-like) transition state found substantial $\pi^+-\pi$ interactions between BMIM and leaving group, with distances of ∼3.5 to 5 Å and angles indicative of sandwich-like conformations. Conversely, the transition state $\pi^+-\pi$ interactions for 2-(4-nitrophenoxy)-3-nitrothiophene (ortho-like) were generally longer

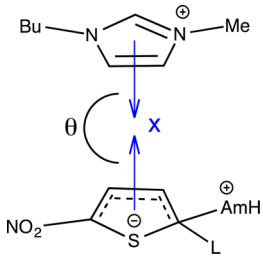


**Figure 2.** Definition of the angle $\theta$ (degrees) and distance $X$ (angstroms) for the $\pi^+-\pi$ interaction between the BMIM cation and a 2-L-5-nitrothiophene (para-like) ring.

**Table 5. Average Distances (Å) and Angles (degrees, given in parentheses) between the Two Nearest BMIM Cations and the para/ortho-like Nitrothiophene Ring or the $OC_6H_4$-4-$NO_2$ Substituent Ring for the Transition State and Intermediate Meisenheimer Complex with the Three Cyclic Amines in [BMIM][$BF_4$][a]**

| para-like | | TS | Meisenheimer |
|---|---|---|---|
| morpholine | nitrothiophene | 5.4 (158), 6.1 (111) | 5.0 (68), 5.1 (115) |
| | $OC_6H_4$-4-$NO_2$ | 3.7 (160), 4.2 (26) | 4.3 (141), 6.2 (146) |
| piperidine | nitrothiophene | 5.4 (97), 6.4 (14) | 6.0 (129), 6.1 (76) |
| | $OC_6H_4$-4-$NO_2$ | 3.5 (146), 5.1 (72) | 5.4 (162), 5.5 (34) |
| pyrrolidine | nitrothiophene | 4.9 (128), 5.9 (85) | 4.5 (54), 5.5 (90) |
| | $OC_6H_4$-4-$NO_2$ | 3.9 (139), 4.4 (161) | 4.3 (139), 5.1 (154) |
| ortho-like | | TS | Meisenheimer |
| morpholine | nitrothiophene | 5.4 (74), 5.5 (146) | 5.4 (75), 5.6 (121) |
| | $OC_6H_4$-4-$NO_2$ | 5.8 (94), 6.1 (69) | 3.6 (141), 3.9 (158) |
| piperidine | nitrothiophene | 4.9 (103), 6.1 (15) | 5.1 (44), 6.0 (99) |
| | $OC_6H_4$-4-$NO_2$ | 6.1 (25), 6.2 (128) | 5.1 (92), 5.6 (35) |
| pyrrolidine | nitrothiophene | 5.5 (131), 5.8 (134) | 6.0 (88), 6.2 (17) |
| | $OC_6H_4$-4-$NO_2$ | 3.7 (147), 4.7 (132) | 4.8 (130), 5.1 (166) |

[a]See Figure 2 for the definition of the distance and angle between aromatic rings.

with distances of roughly 5 to 6 Å between the leaving group and BMIM, and they featured a more T-shaped orientation, that is, angles closer to 90°. The BMIM interactions with the nitrothiophene ring were very similar in both the para-like and ortho-like 4-nitrophenoxy-nitrothiophene systems, for example, distances of 5 to 6 Å. The intermediate Meisenheimer complexes for each cyclic amine reaction showed a similar trend to the transition state but with slightly longer distances of ∼4−6 Å between the BMIM and 4-nitrophenoxy substituent (Table 5).

**Charges.** Selected scaled CM3 charges from the QM/MM/MC calculations show that the higher electronegativity of the oxygen atom from the methoxy, phenoxy, and 4-nitrophenoxy substituents draws a greater amount of electron density from ipso

**Table 4. Dihedral Angles Φ (degrees) for the Transition Structures Between Piperidine and the 2-L-3-Nitrothiophene (ortho-like) and 2-L-5-Nitrothiophene (para-like) Isomers at 25 °C in Solution[a]**

| nucleophile | thiophene derivative | leaving group (L) | Φ $CH_3OH$ | Φ [BMIM][$BF_4$] | Φ [BMIM][$PF_6$] |
|---|---|---|---|---|---|
| piperidine | ortho-like | $OC_6H_5$ | 91 | 48 | 47 |
| | | $OC_6H_4$-4-$NO_2$ | 62 | 77 | 39 |
| | para-like | $OC_6H_5$ | 132 | 199 | 208 |
| | | $OC_6H_4$-4-$NO_2$ | 154 | 206 | 198 |

[a]See Figure 1 for definition of Φ. PDDDG/PM3 and MC/FEP. Angles averaged over the final 5 and 20 million MC configurations in methanol and the ionic liquids, respectively.


dx.doi.org/10.1021/jp504967r | J. Phys. Chem. B XXXX, XXX, XXX−XXX

**Table 6. Selected Atomic Charges (e units) for the 2-L-5-Nitrothiophene (para-like) and Piperidine Transition Structure and Meisenheimer Intermediate Reacting ipso C, Amine N, and Leaving Group O/Br in Solution**

| piperidine | leaving group (L) | C, N, O/Br $CH_3OH$ | C, N, O/Br [BMIM][$BF_4$] | C, N, O/Br [BMIM][$PF_6$] |
|---|---|---|---|---|
| transition | Br | −0.09, −0.45, 0.01 | −0.07, −0.27, −0.01 | −0.09, −0.42, 0.06 |
| structure | $OCH_3$ | 0.16, −0.41, −0.22 | 0.19, −0.34, −0.24 | 0.21, −0.37, −0.30 |
| | $OC_6H_5$ | 0.20, −0.47, −0.21 | 0.12, −0.31, −0.23 | 0.19, −0.37, −0.22 |
| | $OC_6H_4$-4-$NO_2$ | 0.16, −0.45, −0.18 | 0.19, −0.38, −0.26 | 0.16, −0.25, −0.21 |
| Meisenheimer | Br | −0.12, −0.02, −0.08 | −0.07, 0.01, −0.25 | −0.09, 0.05, −0.13 |
| intermediate | $OCH_3$ | 0.11, −0.02, −0.30 | 0.11, −0.06, −0.31 | 0.06, 0.03, −0.32 |
| | $OC_6H_5$ | 0.17, −0.09, −0.32 | 0.16, −0.03, −0.24 | 0.13, 0.09, −0.29 |
| | $OC_6H_4$-4-$NO_2$ | 0.16, −0.07, −0.30 | 0.20, −0.11, −0.30 | 0.18, −0.09, −0.27 |

carbon compared with Br (Tables 6 and Tables S14 and S15 in the Supporting Information). The resultant larger positive charge on the C should favor the nucleophilic attack and enhance the reaction rate of the addition step.

**Amine Nucleophilicity.** The effective nucleophilicity of the amines, which may be directly manipulated by the ionic liquids,[36] should also play a major role in the $S_NAr$ reactivity. For example, the reported nucleophilicity order of Pyr ≥ Pip > Mor is similar in both methanol and [BMIM][$BF_4$], yet the reaction rate for 2-bromo-5-nitrothiophene is enhanced in the ionic liquid with Pyr/Pip/Mor values of 21.8:10.9:1 compared with 5.8:3.7:1 in methanol.[14] In addition, increased rates of reaction have been linked to a decrease in solvation of amines by ionic liquids in previous base-catalyzed heterocyclic rearrangements.[37] This correlation between rate enhancement and nucleophile solvation can be related to the Kamlet−Taft solvent parameters. For example, methanol has a 1.05 hydrogen bond acidity that is nearly double that of 0.627 for [BMIM][$BF_4$] or 0.634 for [BMIM][$PF_6$].[38,39] In addition, the hydrogen bond basicity for methanol is double that of [BMIM][$BF_4$] and [BMIM][$PF_6$], that is, 0.61, 0.376, and 0.207, respectively.[38,39] The hydrogen bond acceptor site of the solvent, that is, anions for the ionic liquids, should be the preferred interaction with the proton on the amine. Amine−solvent interactions have been quantified here by performing QM/MM/MC simulations for each amine solely in a periodic box of solvent and then analyzing the solute−solvent energy pair distributions.

Energy pair distributions record the average number of ions in the ionic liquids or molecules for methanol that interact with the cyclic amines. The plot for Pyr, Pip, and Mor in [BMIM][$BF_4$] is given in Figure 3, whereas the plots in methanol and [BMIM][$PF_6$] are given in the Supporting Information Figures S1 and S2. Highly favorable electrostatic interactions between the amine and solvent components are reflected in the left-most region. A large band centered at 0 kcal/mol arises from the many ions in the outer solvation shells. Examination of the energy pair distributions finds the interaction energy for morpholine has a higher, more favorable peak as compared with either piperidine or pyrrolidine. Accordingly, integration of the curves from −10.0 to −2.0 (or −1.5) kcal/mol finds a greater number of interactions occurring for morpholine than for piperidine or pyrrolidine in the ionic liquids and methanol (Table 7). However, the overall solute−solvent interaction energies are weak because hydrogen bonding in protic solvents tends to have energies more attractive than −5 kcal/mol.[18] The results are consistent with the experimental order of nucleophilicity, that is, Pyr ≥ Pip > Mor.

Detailed examination of the average interaction distances over the final 20 million QM/MM/MC configurations between the [BMIM][$BF_4$] ions and cyclic amines is given in the Supporting Information Tables S16−S18. For example, morpholine was found to have favorable electrostatic interactions with four unique BMIM cations within a 4 Å distance (Table S16 in the Supporting Information). In contrast, pyrrolidine and piperidine interacted with far fewer ions, generally 1 BMIM cation and 1 $BF_4$ anion within 4 Å (Tables S17 and S18 in the Supporting Information). The closest interactions between the [BMIM][$BF_4$] ions and morpholine came between the most acidic protons located on the imidazolium ring, that is, on the 2- and 5-position carbon atoms, and the oxygen on morpholine with distances of 2.51 and 2.88 Å, respectively. The same acidic protons interacted with the nitrogen atom on morpholine, albeit with longer distances of 3.5 to 3.8 Å. For pyrrolidine, the most acidic imidazolium two-position proton ($pK_a$ = 21−23)[40,41] interacted with the amine nitrogen atom at a distance of 2.81 Å. In addition, a $BF_4$ anion interacted with the hydrogen atom bonded to the pyrrolidine nitrogen at a distance of 3.46 Å. Average distances between the [BMIM][$PF_6$] ions and the cyclic amines (given in Supporting Information Tables S19−S21) followed the same general trend as [BMIM][$BF_4$] and were consistent with Table 7. In methanol, despite a lower number of solvent molecules interacting with the

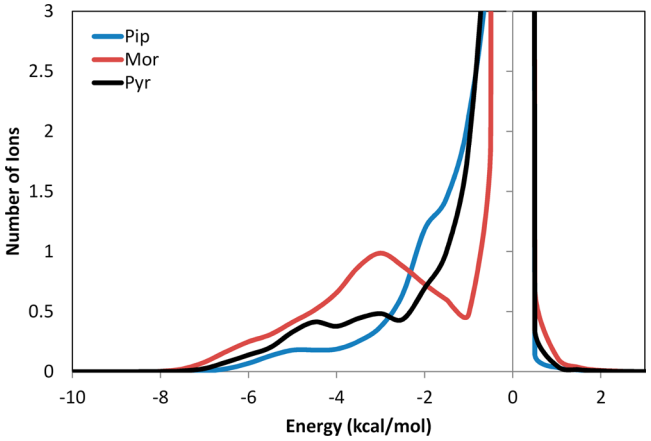


**Figure 3.** Solute−solvent energy pair distributions for piperidine, morpholine, and pyrrolidine in [BMIM][$BF_4$] at 25 °C.

**Table 7. Solute−Solvent Energy Pair Distributions for the Morpholine, Piperidine, and Pyrrolidine in Methanol and Ionic Liquids Integrated to −2.0 kcal/mol (and −1.5 kcal/mol in parentheses)[a]**

| | MeOH | [BMIM][$BF_4$] | [BMIM][$PF_6$] |
|---|---|---|---|
| morpholine | 2.4 (4.6) | 5.9 (6.5) | 5.3 (6.4) |
| piperidine | 1.3 (2.2) | 3.2 (4.7) | 5.2 (6.1) |
| pyrrolidine | 0.4 (1.7) | 3.6 (4.6) | 3.9 (4.5) |

[a]From Figure 3 and Figures S1 and S2 in the Supporting Information.


dx.doi.org/10.1021/jp504967r | J. Phys. Chem. B XXXX, XXX, XXX−XXX

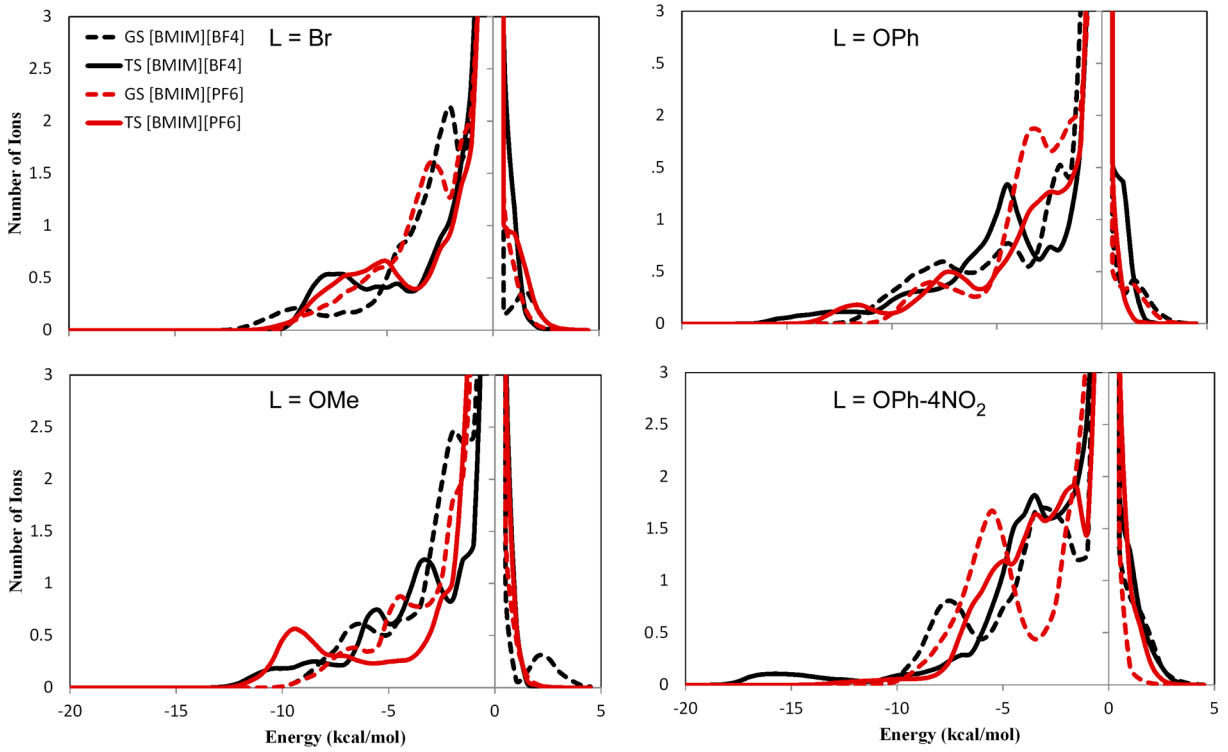


**Figure 4.** Solute−solvent energy pair distributions for $S_NAr$ reaction between piperidine and 2-L-5-nitrothiophene in [BMIM][$BF_4$] and [BMIM][$PF_6$] at 25 °C. Transition structures as solid lines and reactants as dashed lines.

**Table 8. Solute−Solvent Energy Pair Distributions for the $S_NAr$ Reactions between the 2-L-3-Nitrothiophene (ortho-like) and 2-L-5-Nitrothiophene (para-like) Isomers and Three Cyclic Amines in Methanol and Ionic Liquids Integrated to −3.5 kcal/mol for the Transition State[a]**

| nucleophile | thiophene derivative | leaving group (L) | $CH_3OH$ | [BMIM][$BF_4$] | [BMIM][$PF_6$] |
|---|---|---|---|---|---|
| morpholine | ortho-like | Br | 3.7 (3.3) | 5.8 (7.1) | 6.3 (5.8) |
| | | $OCH_3$ | 4.7 (5.3) | 6.8 (5.8) | 7.9 (7.3) |
| | | $OC_6H_5$ | 4.2 (5.2) | 7.5 (7.2) | 7.5 (9.5) |
| | | $OC_6H_4$-4-$NO_2$ | 5.4 (5.8) | 8.6 (8.8) | 9.2 (11.5) |
| | para-like | Br | 3.5 (2.9) | 6.9 (5.8) | 7.4 (5.2) |
| | | $OCH_3$ | 4.2 (4.8) | 7.0 (8.5) | 8.4 (6.7) |
| | | $OC_6H_5$ | 5.4 (5.0) | 9.4 (10.7) | 8.8 (9.0) |
| | | $OC_6H_4$-4-$NO_2$ | 4.4 (5.1) | 9.8 (10.1) | 9.4 (9.6) |
| piperidine | ortho-like | Br | 6.4 (2.3) | 6.9 (4.9) | 7.2 (6.8) |
| | | $OCH_3$ | 3.3 (4.3) | 6.1 (7.0) | 6.6 (7.2) |
| | | $OC_6H_5$ | 3.2 (4.7) | 7.8 (8.4) | 8.2 (7.7) |
| | | $OC_6H_4$-4-$NO_2$ | 5.1 (4.7) | 8.9 (8.9) | 8.6 (9.1) |
| | para-like | Br | 2.9 (3.5) | 5.2 (5.5) | 5.7 (6.4) |
| | | $OCH_3$ | 4.6 (2.6) | 7.3 (5.9) | 5.3 (5.4) |
| | | $OC_6H_5$ | 3.6 (3.1) | 9.6 (8.1) | 7.1 (7.8) |
| | | $OC_6H_4$-4-$NO_2$ | 5.1 (4.2) | 9.8 (9.4) | 9.5 (10.0) |
| pyrrolidine | ortho-like | Br | 2.2 (3.9) | 5.4 (6.6) | 5.3 (5.9) |
| | | $OCH_3$ | 1.8 (3.0) | 6.5 (5.8) | 6.7 (5.6) |
| | | $OC_6H_5$ | 2.0 (4.2) | 6.8 (7.9) | 7.5 (7.3) |
| | | $OC_6H_4$-4-$NO_2$ | 2.6 (5.9) | 7.5 (9.1) | 7.5 (9.1) |
| | para-like | Br | 3.2 (4.8) | 5.9 (4.9) | 6.4 (4.9) |
| | | $OCH_3$ | 4.3 (2.7) | 7.4 (6.8) | 5.7 (6.9) |
| | | $OC_6H_5$ | 3.9 (3.1) | 9.5 (9.7) | 8.9 (10.2) |
| | | $OC_6H_4$-4-$NO_2$ | 4.4 (4.5) | 10.0 (8.3) | 9.4 (10.9) |

[a]Reactants are given in parentheses.

amines, the solute−solvent interactions are far more energetically favorable with higher values, for example, −8 to −9 kcal/mol (Figure S1 in the Supporting Information), compared with the ionic liquids with average values around −2 to −6 kcal/mol. The results are consistent with an enhanced nucleophilicity of the cyclic amines in the ionic liquids relative to methanol.


dx.doi.org/10.1021/jp504967r | J. Phys. Chem. B XXXX, XXX, XXX−XXX

**Transition State.** Solute−solvent energy pair distributions were computed in the representative FEP windows near the reactants and the addition step transition state for all reaction combinations in the ionic liquids (Figures 4 and Figures S3−S22 in the Supporting Information). The $S_NAr$ reactions had distributions with lower energies and smaller peaks at the ground state in general when compared with the corresponding transition state (Table 8). For instance, integration of the distributions from −20.0 to −3.5 kcal/mol for the reaction between piperidine and 2-methoxy-5-nitrothiophene in [BMIM][$BF_4$] found more favorable ions complexing to the transition structures compared with the reactants, that is, 7.3 and 5.9 ions, respectively. The trend is not always exclusive as the same reaction in [BMIM][$PF_6$] found a similar number of ions for the transition state and reactants, that is, 5.3 and 5.4, respectively. Multiple cases (Table 8) found the opposite result, highlighting the complex charge interactions developing throughout the reaction pathway. In general, the amine proton was electrostatically stabilized by a $BF_4$ anion, whereas the oxygen or bromine leaving groups formed hydrogen bonds with protons located on the imidazolium cations. For example, in the case of piperidine and 2-methoxy-5-nitrothiophene, the methoxy group interacted with the cation's hydrogen atoms on the terminal butyl chain carbons. However, the [BMIM]'s more acidic protons located on the four- and five-positions interacted when the full charge separation emerged in the Meisenheimer intermediate (Figure 5). The

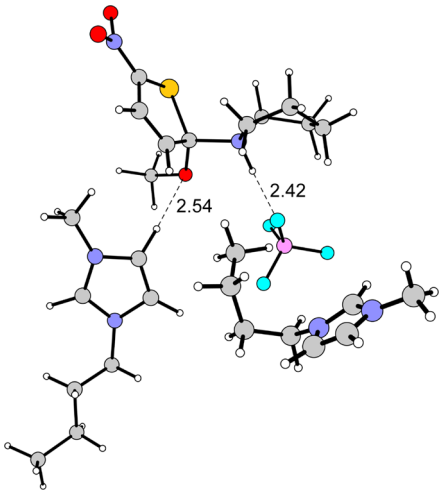


**Figure 5.** Typical snapshot of the Meisenheimer intermediate between piperidine and 2-methoxy-5-nitrothiophene in [BMIM][$BF_4$]. The distances (angstroms) are average values over the final 20 million configurations of QM/MM/MC simulations. Only nearby ions are retained for clarity.

structural and electronic similarities between the transition structures and intermediates are indicated by the low computed $\Delta G^{\ddagger}_{reverse}$ values (Table 3).

The encapsulation of the addition step transition state and the Meisenheimer intermediate between piperidine and 2-methoxy-5/3-nitrothiophene (para- and ortho-like) by the [BMIM][$BF_4$] ionic liquid has been investigated in detail and is representative of the other cyclic amines and ionic liquids. For the reaction between piperidine and the methoxy-based para-like nitrothiophene, there are eight to nine ions that are within 3 Å of the transition state and Meisenheimer intermediate. Figure 5 illustrates a typical snapshot of the most favorable site-specific solute−solvent interactions. All interactions between the ionic liquid ions within ~5.5 Å are given in the Supporting Information (Tables S22−S25). As expected, the charge separation that is developing at the transition state and fully realized at the intermediate is stabilized by the appropriate counterion; for example, in Figure 5, the $BF_4$ anion is closely interacting with the positively charged amine. Figure 6 illustrates how the [BMIM][$BF_4$]

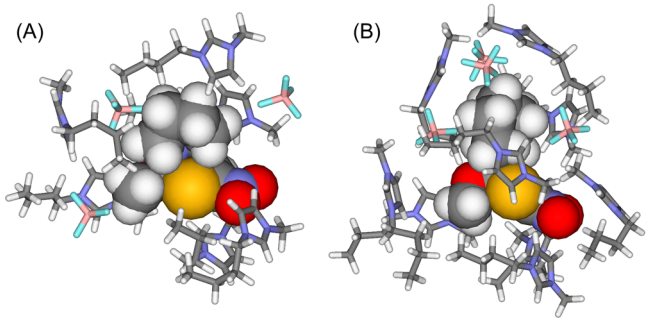


**Figure 6.** Illustration of first-solvation shell [BMIM][$BF_4$] (shown as sticks) encapsulation of the (A) addition transition state and (B) the Meisenheimer intermediate for the $S_NAr$ reaction between piperidine and 2-methoxy-5-nitrothiophene (given as CPK space-filling model).

ions form a cage-like structure to favorably interact with the substrates. The calculations found the degree of ordering to increase as the charge separation increases. The findings correlated well with experimental measurements that reported the $S_NAr$ reaction to be entropy-disfavored in every case relative to methanol.[14] Interestingly, the Meisenheimer complex featured a cage-like liquid clathrate structure similar to experimental reports of liquid clathrate formation in 1-alkyl-3-methylimidazolium-based ionic liquids with aromatic compounds.[42] Despite the entropy penalty, the ordered ionic liquid structure provided significantly reduced activation enthalpy values for the same reaction in methanol, for example, experimental $\Delta H^{\ddagger}$ of ~5 kcal/mol lower.[14]

Enhancements in the rate of reaction correlate well with an increase in the medium polarizability, which should better stabilize the polar transition structures. For example, the lower $\Delta G^{\ddagger}$ in the ionic liquids are consistent with dipolarity/polarizability Kamlet−Taft parameter because [BMIM][$BF_4$] and [BMIM][$PF_6$] have a $\pi^*$ of 1.047 and 1.032, respectively, compared with 0.73 in methanol.[38,39] Similar findings have been reported for aliphatic nucleophilic substitution reactions in the presence of neutral nucleophiles such as amines.[36]

## CONCLUSIONS

In summary, QM/MM MC/FEP calculations have been performed on $S_NAr$ reactions between cyclic secondary amines (i.e., piperidine, pyrrolidine, and morpholine) and the 2-L-5-nitrothiophene (para-like) or 2-L-3-nitrothiophene (ortho-like) isomers, where L = bromo, methoxy, phenoxy, and 4-nitrophenoxy. D'Anna et al. reported an enhanced reactivity derived from the ionic liquids [BMIM][$BF_4$] and [BMIM][$PF_6$] relative to conventional solvents.[14] Accordingly, the QM/MM calculations featuring hundreds of explicit solvent molecules/ions reproduced the experimentally observed free energies of activation reasonably well when considering error bars in the calculation and experiment in both methanol and the ionic liquids.

Beneficial ionic liquid effects on $S_NAr$ reactivity can be attributed to a combination of factors including (1) an enhanced


dx.doi.org/10.1021/jp504967r | J. Phys. Chem. B XXXX, XXX, XXX−XXX

nucleophilicity of the cyclic amines with an order of Pyr ≥ Pip > Mor, (2) favorable $\pi^+-\pi$ interactions between the BMIM cations and the aromatic rings present on the substrate, and (3) significant electrostatic enhancements between the solvent and the developing charge separation forming at the transition state (and at the intermediate Meisenheimer complex) compared with the reactants. A highly ordered ionic liquid clathrate formation was found to deliver site-specific hydrogen bonding stabilization that, despite an entropy penalty, provided a reduction in the activation barriers. Overall, deeper insight into the effect of the ionic liquids upon the $S_NAr$ has been provided, and many of the observations should be applicable toward understanding the role of solvent on other important addition/elimination reaction types.

## ■ ASSOCIATED CONTENT

### Supporting Information

Additional figures for charges and transition states in solution; solute−solvent energy pair distributions; hydrogen bond distances between ions and solute at the transition and ground states; $\pi^+-\pi$ interaction distances and angles; DFT energies, frequencies, and coordinates of structures; and complete ref 31. This material is available free of charge via the Internet at http://pubs.acs.org.

## ■ AUTHOR INFORMATION


### Corresponding Author

*E-mail: orlando.acevedo@auburn.edu.


### Notes

The authors declare no competing financial interest.

## ■ ACKNOWLEDGMENTS

Gratitude is expressed to the National Science Foundation (CHE-1149604) and the Alabama Supercomputer Center for support of this research.

## ■ REFERENCES


(1) Freemantle, M. *An Introduction to Ionic Liquids*; RSC Publishing: Cambridge, U.K., 2009.

(2) Castner, E. W.; Wishart, J. F.; Shirota, H. Intermolecular Dynamics, Interactions, and Solvation in Ionic Liquids. *Acc. Chem. Res.* **2007**, *40*, 1217−1227.

(3) Iwata, K.; Okajima, H.; Saha, S.; Hamaguchi, H. Local Structure Formation in Alkyl-Imidazolium-Based Ionic Liquids as Revealed by Linear and Nonlinear Raman Spectroscopy. *Acc. Chem. Res.* **2007**, *40*, 1174−1181.

(4) Weingaertner, H. Understanding Ionic Liquids at the Molecular Level: Facts, Problems, and Controversies. *Angew. Chem., Int. Ed.* **2008**, *47*, 654−670.

(5) Anderson, J. L.; Ding, J.; Welton, T.; Armstrong, D. W. Characterizing Ionic Liquids on the Basis of Multiple Solvation Interactions. *J. Am. Chem. Soc.* **2002**, *124*, 14247−14254.

(6) Pârvulescu, V. I.; Hardacre, C. Catalysis in Ionic Liquids. *Chem. Rev.* **2007**, *107*, 2615−2665.

(7) van Rantwijk, F.; Sheldon, R. A. Biocatalysis in Ionic Liquids. *Chem. Rev.* **2007**, *107*, 2757−2785.

(8) Welton, T. Ionic Liquids in Catalysis. *Coord. Chem. Rev.* **2004**, *248*, 2459−2477.

(9) Hallett, J. P.; Welton, T. Room-Temperature Ionic Liquids: Solvents for Synthesis and Catalysis. 2. *Chem. Rev.* **2011**, *111*, 3508−3576.

(10) Zhang, Z. C. Catalysis in Ionic Liquids. *Adv. Catal.* **2006**, *49*, 153−237.

(11) Welton, T. Room-Temperature Ionic Liquids. Solvents for Synthesis and Catalysis. *Chem. Rev.* **1999**, *99*, 2071−2083.

(12) Parker, A. J. Protic-Dipolar Aprotic Solvent Effects on Rates of Bimolecular Reactions. *Chem. Rev.* **1969**, *69*, 1−32.

(13) Acevedo, O.; Jorgensen, W. L. Solvent Effects and Mechanism for a Nucleophilic Aromatic Substitution from QM/MM Simulations. *Org. Lett.* **2004**, *6*, 2881−2884.

(14) D'Anna, F.; Frenna, V.; Noto, R.; Pace, V.; Spinelli, D. Study of Aromatic Nucleophilic Substitution with Amines on Nitrothiophenes in Room-Temperature Ionic Liquids: Are the Different Effects on the Behavior of Para-Like and Ortho-Like Isomers on Going from Conventional Solvents to Room-Temperature Ionic Liquids Related to Solvation Effects? *J. Org. Chem.* **2006**, *71*, 5144−5150.

(15) D'Anna, F.; Marullo, S.; Noto, R. Ionic Liquids/[Bmim][N3] Mixtures: Promising Media for the Synthesis of Aryl Azides by SNAr. *J. Org. Chem.* **2008**, *73*, 6224−6228.

(16) Spinelli, D.; Consiglio, G.; Noto, R. Catalysis in Aromatic Nucleophilic Substitution. 3. Reactions of Piperidine with 2-Methoxy-3-Nitrothiophene and 2-Methoxy-5-Nitrothiophene in Methanol. *J. Org. Chem.* **1978**, *43*, 4038−4041.

(17) Bernasconi, C. F.; De Rossi, R. H. Influence of the O-Nitro Group on Base Catalysis in Nucleophilic Aromatic Substitution. Reactions in Benzene Solution. *J. Org. Chem.* **1976**, *41*, 44−49.

(18) Acevedo, O.; Jorgensen, W. L. Influence of Inter- and Intramolecular Hydrogen Bonding on Kemp Decarboxylations from QM/MM Simulations. *J. Am. Chem. Soc.* **2005**, *127*, 8829−8834.

(19) Repasky, M. P.; Chandrasekhar, J.; Jorgensen, W. L. PDDG/PM3 and PDDG/MNDO: Improved Semiempirical Methods. *J. Comput. Chem.* **2002**, *23*, 1601−1622.

(20) Tubert-Brohman, I.; Guimarães, C. R. W.; Repasky, M. P.; Jorgensen, W. L. Extension of the PDDG/PM3 and PDDG/MNDO Semiempirical Molecular Orbitial Methods to the Halogens. *J. Comput. Chem.* **2003**, *25*, 138−150.

(21) Tubert-Brohman, I.; Guimarães, C. R. W.; Jorgensen, W. L. Extension of the PDDG/PM3 Semiempirical Molecular Orbital Method to Sulfur, Silicon, and Phosphorus. *J. Chem. Theory Comput.* **2005**, *1*, 817−823.

(22) Acevedo, O.; Jorgensen, W. L. Advances in Quantum and Molecular Mechanical (QM/MM) Simulations for Organic and Enzymatic Reactions. *Acc. Chem. Res.* **2010**, *43*, 142−151.

(23) Acevedo, O.; Armacost, K. Claisen Rearrangements: Insight into Solvent Effects and "on Water" Reactivity from QM/MM Simulations. *J. Am. Chem. Soc.* **2010**, *132*, 1966−1975.

(24) Sheppard, A. N.; Acevedo, O. Multidimensional Exploration of Valley-Ridge Inflection Points on Potential Energy Surfaces. *J. Am. Chem. Soc.* **2009**, *131*, 2530−2540.

(25) Acevedo, O.; Jorgensen, W. L.; Evanseck, J. D. Elucidation of Rate Variations for a Diels-Alder Reaction in Ionic Liquids from QM/MM Simulations. *J. Chem. Theory. Comput.* **2007**, *3*, 132−138.

(26) Acevedo, O.; Jorgensen, W. L. Understanding Rate Accelerations for Diels-Alder Reactions in Solution Using Enhanced QM/MM Methodology. *J. Chem. Theory Comput.* **2007**, *3*, 1412−1419.

(27) Sambasivarao, S. V.; Acevedo, O. Development of OPLS-AA Force Field Parameters for 68 Unique Ionic Liquids. *J. Chem. Theory Comput.* **2009**, *5*, 1038−1050.

(28) Allen, C.; Sambasivarao, S. V.; Acevedo, O. An Ionic Liquid Dependent Mechanism for Base Catalyzed $\beta$-Elimination Reactions from QM/MM Simulations. *J. Am. Chem. Soc.* **2013**, *135*, 1065−1072.

(29) Thompson, J. D.; Cramer, C. J.; Truhlar, D. G. Parameterization of Charge Model 3 for AM1, PM3, BLYP, and B3LYP. *J. Comput. Chem.* **2003**, *24*, 1291−1304.

(30) Vilseck, J. Z.; Sambasivarao, S. V.; Acevedo, O. Optimal Scaling Factors for CM1 and CM3 Atomic Charges in Aqueous RM1-Based Simulations. *J. Comput. Chem.* **2011**, *32*, 2836−2842.

(31) Frisch, M. J. *Gaussian 09*, revision D.01; Gaussian: Wallingford, CT, 2013.

(32) Cossi, M.; Rega, N.; Scalmani, G.; Barone, V. Achieving Linear-Scaling Computational Cost for the Polarizable Continuum Model of Solvation. *J. Comput. Chem.* **2003**, *24*, 669−681.

(33) Hermans, J.; Wang, L. Inclusion of Loss of Translational and Rotational Freedom in Theoretical Estimates of Free Energies of

Binding. Application to a Complex of Benzene and Mutant T4 Lysozyme. *J. Am. Chem. Soc.* **1997**, *119*, 2707−2714.
(34) D'Anna, F.; Frenna, V.; Pace, V.; Noto, R. Effect of Ionic Liquid Organizing Ability and Amine Structure on the Rate and Mechanism of Base Induced Elimination of 1,1,1-Tribromo-2,2-Bis(Phenyl-Substituted)Ethane. *Tetrahedron* **2006**, *62*, 1690−1698.
(35) D'Anna, F.; Marullo, S.; Vitale, P.; Noto, R. Electronic and Steric Effects: How Do They Work in Ionic Liquids? The Case of Benzoic Acid Dissociation. *J. Org. Chem.* **2010**, *75*, 4828−4834.
(36) Crowhurst, L.; Lancaster, N. L.; Arlandis, J. M. P.; Welton, T. Manipulating Solute Nucleophilicity with Room Temperature Ionic Liquids. *J. Am. Chem. Soc.* **2004**, *126*, 11549−11555.
(37) D'Anna, F.; Frenna, V.; Noto, R.; Pace, V.; Spinelli, D. Can the Absence of Solvation of Neutral Reagents by Ionic Liquids Be Responsible for the High Reactivity in Base-Assisted Intramolecular Nucleophilic Substitutions in These Solvents? *J. Org. Chem.* **2005**, *70*, 2828−2831.
(38) Crowhurst, L.; Mawdsley, P. R.; Perez-Arlandis, J. M.; Salter, P. A.; Welton, T. Solvent−Solute Interactions in Ionic Liquids. *Phys. Chem. Chem. Phys.* **2003**, *5*, 2790−2794.
(39) Kamlet, M. J.; Abboud, J. L. M.; Abraham, M. H.; Taft, R. W. Linear Solvation Energy Relationships. 23. A Comprehensive Collection of the Solvatochromic Parameters, .Pi.*, .Alpha., and .Beta., and Some Methods for Simplifying the Generalized Solvatochromic Equation. *J. Org. Chem.* **1983**, *48*, 2877−2887.
(40) Amyes, T. L.; Diver, S. T.; Richard, J. P.; Rivas, F. M.; Toth, K. Formation and Stability of N-Heterocyclic Carbenes in Water: The Carbon Acid pKa of Imidazolium Cations in Aqueous Solution. *J. Am. Chem. Soc.* **2004**, *126*, 4366−4374.
(41) Dupont, J.; Spencer, J. On the Noninnocent Nature of 1,3-Dialkylimidazolium Ionic Liquids. *Angew. Chem., Int. Ed.* **2004**, *43*, 5296−5297.
(42) Holbrey, J. D.; Reichert, W. M.; Nieuwenhuyzen, M.; Sheppard, O.; Hardacre, C.; Rogers, R. D. Liquid Clathrate Formation in Ionic Liquid-Aromatic Mixtures. *Chem. Commun.* **2003**, 476−477.